Langmuir

Article

pubs.acs.org/Langmuir

Effect of Laundry Surfactants on Surface Charge and Colloidal Stability of Silver Nanoparticles

Sara Skoglund,*[,†] Troy A. Lowe,[†,‡] Jonas Hedberg,[†] Eva Blomberg,*[,†,§] Inger Odnevall Wallinder,[†] Susanna Wold,[‡] and Maria Lundin[†,‡]

KTH Royal Institute of Technology, School of Chemical Science and Engineering, [†]Surface and Corrosion Science, and [‡]Applied Physical Chemistry, SE-100 44 Stockholm, Sweden

[§]Chemistry, Materials and Surfaces, SP Technical Research Institute of Sweden, Box 5607, SE-114 86 Stockholm, Sweden

Supporting Information

ABSTRACT: The stability of silver nanoparticles (Ag NPs) potentially released from clothing during a laundry cycle and their interactions with laundry-relevant surfactants [anionic (LAS), cationic (DTAC), and nonionic (Berol)] have been investigated. Surface interactions between Ag NPs and surfactants influence their speciation and stability. In the absence of surfactants as well as in the presence of LAS, the negatively charged Ag NPs were stable in solution for more than 1 day. At low DTAC concentrations (≤1 mM), DTAC−Ag NP interactions resulted in charge neutralization and formation of agglomerates. The surface charge of the particles became positive at higher concentrations due to a bilayer type formation of DTAC that prevents from agglomeration due to repulsive electrostatic forces between the positively charged colloids. The adsorption of Berol was enhanced when above its critical micelle concentration (cmc). This resulted in a surface charge close to zero and subsequent agglomeration. Extended DLVO theory calculations were in compliance with observed findings. The stability of the Ag NPs was shown to depend on the charge and concentration of the adsorbed surfactants. Such knowledge is important as it may influence the subsequent transport of Ag NPs through different chemical transients and thus their potential bioavailability and toxicity.

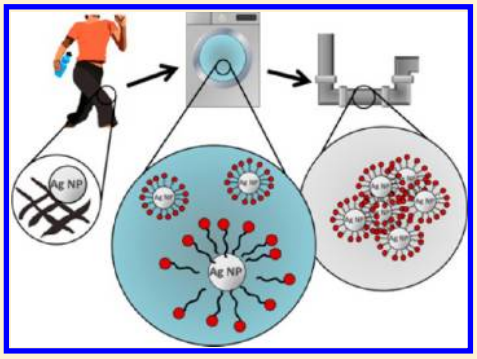

1. INTRODUCTION

Silver nanoparticles (Ag NPs) are, due to their antibacterial properties, very commonly used in consumer products such as textiles, plastics, creams, and cosmetics.[1−3] A rapid increase of use will inevitably result in increased Ag concentrations in the sludge at the wastewater treatment plants (WWTP) and eventually on arable land.[4] Since Ag is toxic for aquatic organisms such as fish, and may result in antibiotic resistance for bacteria, an in-depth understanding of the environmental fate of Ag released from consumer products (as NPs or ions) into different aquatic transients is needed.[1] Sport clothing is a large market for Ag NPs.[3,5,6] However, recent studies have shown that almost all impregnated Ag in sports socks may be released already during the first few washing cycles in deionized water[3] and in a simulated washing cycle with surfactants.[5] These studies did not, however, investigate any interaction between Ag NPs and the laundry surfactants. Previous studies by the authors have shown such interactions to be highly surfactant-specific.[7] Colloidal stability and stability of the chemical form (essential for bioavailability and toxicity) of released Ag and/or Ag NPs when discharged from the washing machine into the wastewater system will govern their mobility and further transport to subsequent chemical transients and finally to the WWTP.[8,9] Changes in chemical conditions of different transients will inevitably result in possible changes in speciation. The colloidal mobility depends on size and surface characteristics including surface charge distribution, which is directly connected to the chemical form of Ag. Transportation will also take place as long as the particles are stable in solution.[10−14]

Ag NPs are often synthesized in the presence of capping agents, such as surfactants or polymers,[11,15] to prevent particle agglomeration and obtain as monodisperse solutions as possible. Colloidal stability measurements of such synthesized NPs are reported for aqueous solutions of varying ionic strength, acidity, and presence of organic species.[11,14,16−19] Since the stability of NPs is ligand-specific, noncapped NPs may not behave in the same way. It is hence important to investigate the colloidal stability for system-specific conditions.

The aim of this study has been to investigate the colloid stability of laser ablated Ag NPs in aqueous solutions of pH 10 equilibrated with surfactants of various concentrations of relevance for laundry formulations and at subsequent interactions with deionized water (pH 5.6). The Ag NP concentration chosen (1−3 mg/L) mimics findings from release studies of Ag NPs from sport socks during a washing cycle.[3] Two common surfactants of laundry formulations, the negatively charged sodium dodecylbenzenesulfonate, LAS, and

Received: April 4, 2013
Revised: June 12, 2013
Published: June 12, 2013

   dx.doi.org/10.1021/la4012873 | Langmuir 2013, 29, 8882−8891

nonionic Berol 266, Berol, were selected for investigation.[20] The interaction of positively charged surfactants was also investigated as they often are used in softeners. Positively charged dodecyl trimethylammonium chloride, DTAC, was selected as a model component since it has the same chain length as LAS and properties resembling surfactants used in fabric softeners. A multianalytical approach was employed, combining dynamic light scattering (DLS), ζ-potential measurements, and adsorption studies with quartz crystal microbalance with dissipation (QCM-D). This enabled in-depth studies of the kinetics of colloidal stability and changes in size distribution and surface charge upon surfactant−Ag NP interactions. DLS was performed using photon cross-correlation spectroscopy (PCCS). The particles in solution were characterized by means of transmission electron microscopy (TEM). Atomic absorption spectroscopy (AAS) was used to determine the total silver concentration in solution.

2. MATERIAL AND METHODS

2.1. Particles, Surfactants, and Solutions. Ag NPs, produced by laser ablation, were purchased from EV Nano Technology Company Ltd., China, with a specified mean particle diameter of 10 nm. The powder was investigated as-received, at a concentration of 3 mg/L in deionized water (pH 5.6) and at 1 mg/L in synthetic laundry-relevant water solutions (pH 10, 2 mM Na_2CO_3 adjusted to pH 10 by HNO_3). These particle concentrations were similar to measured Ag concentrations in the laundry water (up to 1.3 mg/L) released from Ag-impregnated clothing.[3] The particle suspensions were freshly prepared by dispersing 1 g/L Ag NPs in the relevant solution followed by sonication (5 min, Branson sonifier 250, 30% duty cycle) and subsequent filtration (0.45 μm cellulose acetate filter, Whatman) to remove large agglomerates and dust from solution. The final particle concentration was determined by means of AAS. All solutions were freshly prepared in ultrapure water (resistivity 18.2 MΩ cm, Millipore Sweden).

The charged surfactants (DTAC and LAS) were purchased from Sigma-Aldrich, Sweden (reagent grade). Berol 266 (Berol), an alcohol ethoxylate with a chain length of C9−11 and 4−7 ethylene oxide groups (molecular weight range of 320−480 g/mol with median 402 g/mol—supplier information), was purchased from Akzo Nobel, Sweden.

The critical micelle concentrations (cmc) in water according to literature values, or supplier information, are approximately 20 (DTAC), 1.2 (LAS), and 0.075 mM (Berol).[20] The cmc was expected to be slightly lower (for LAS and DTAC) in the presence of Na_2CO_3 and HNO_3 (used to adjust the solution pH to 10). The investigated surfactant concentrations were varied between 0.01 and 28 mM to investigate concentrations below and above the cmc of each surfactant. The differently concentrated samples were prepared separately, and not by continuous addition of surfactants to the solution to increase the concentration. The latter preparation procedure has recently been reported to influence the interaction between oppositely charged species and their long-term stability.[21]

2.2. Transmission Electron Microscopy. Transmission electron microscopy (TEM) imaging was performed using a JEOL JEM 2100F instrument operating at 200 kV. The samples were prepared by dispersing 1 g/L Ag NPs in a pH 10 water solution followed by sonication (5 min, Sonifier 250, 30% duty cycle). The solution was then pipetted onto TEM copper grids coated with holey carbon films, and the liquid was evaporated at ambient air conditions (25 °C) leaving the NPs on the support. Measurements were done on both nonfiltered and filtered particle dispersions. Both TEM and scanning transmission electron microscopy (STEM) mode were used to analyze the samples (within an hour from sample preparation). TEM images were recorded in bright field (BF), and STEM images were recorded both in bright field and dark field (DF). Analysis with energy-dispersive X-ray spectroscopy (EDS) was performed in STEM mode.

2.3. Surface Potential. The ζ-potential, related to the surface potential, was determined by means of laser Doppler micro-electrophoresis using a Zetasizer Nano ZS instrument (Malvern Instruments, U.K.) at 25 °C. The results are presented as average values of two replica samples measured twice per sample, if not otherwise stated. Standard latex samples (Malvern Instruments) were tested prior to analysis to ensure the accuracy of the measurements.

2.4. Particle Size Distribution. Particle size distribution measurements were conducted by DLS on an instrument employing PCCS (NanoPhox, Sympatec, Germany). Single samples were measured three times each at 25 °C, and data from the unique measurements was integrated to produce a single distribution with the PCCS software. To verify the results, spot checks were performed on random samples. Standard latex samples (20 ± 2 nm) (Sympatec) and blank samples were tested prior to analysis to ensure the accuracy of the measurements.

2.5. Atomic Absorption Spectroscopy. Determination of total investigated Ag NP concentrations was performed by means of atomic absorption spectroscopy (Perkin-Elmer AAnalyst 800) using a graphite furnace accessory. Calibration was conducted using 30, 200, 500 μg/L Ag standards (Perkin-Elmer). All samples were acidified with 65% HNO_3 to a pH <0.5 before measurement. Triplicate samples were prepared for each Ag NP concentration. Blank (test solution without Ag NPs) and standard samples were measured throughout the analysis and all samples were diluted to fall within the calibration range (30−500 μg/L).

2.6. Quartz Crystal Microbalance. Quartz crystal microbalance measurements were conducted using a QCM-D E4 from Q-sense AB (Sweden). The sensed mass of surfactant molecules onto evaporated Ag surfaces (QSX 322, Biolin AB, Sweden) was estimated with the Sauerbrey equation.[22] Measurements were performed at 25 °C with a continuous surfactant solution flow rate of 200 μL/min during the entire measurement. The QCM Ag surfaces were ultrasonically cleaned for 10 min in isopropyl alcohol followed by 5 min in absolute ethanol prior to use. The surface roughness (R_q equals 3 nm) was estimated by means of atomic force microscopy imaging (tapping mode) using a silicon nitride cantilever (MicroMasch) with a scan size area of 5 μm × 5 μm (see Supporting Information Figure S1).

3. RESULTS AND DISCUSSION

3.1. Silver Particle Characterization. The size and morphology of the Ag NPs were examined by means of TEM (Figure 1, parts a and b, and Figure S2 in the Supporting Information).

Figure 1a shows the TEM image of a probe-sonicated sample in a water solution pH 10, prepared as described in section 2.1, with particles sized approximately 1−10 nm. This is in accordance with measurements by means of PCCS in water solutions of pH 5.6 and pH 10 (1−10 nm, average diameter by number ≈1.6 nm).[7] However, Figure 1 also reveals the existence of larger agglomerates and particles (sized approximately 20−50 nm). To remove the largest agglomerates, the samples were filtered prior to the PCCS measurements. TEM images of filtered solutions showed more monodisperse samples (Figure 1b). These findings demonstrate the importance of preparing all samples, not only the TEM grids, in a solution and experimentally relevant way. Findings on the same particles investigated by means of TEM, but prepared in differently using butanol (cf. Supporting Information Figure S2), show the importance of sonication and filtration on the final result. These observations are consistent with earlier finding.[23]

Particles observed by means of TEM were verified as silver by means of EDS analysis performed in STEM mode, see insets a−c in Figure 1a. A crystalline structure of the particles was discerned (cf. Figure 1b) as well as the absence of an outer

dx.doi.org/10.1021/la4012873 | Langmuir 2013, 29, 8882−8891

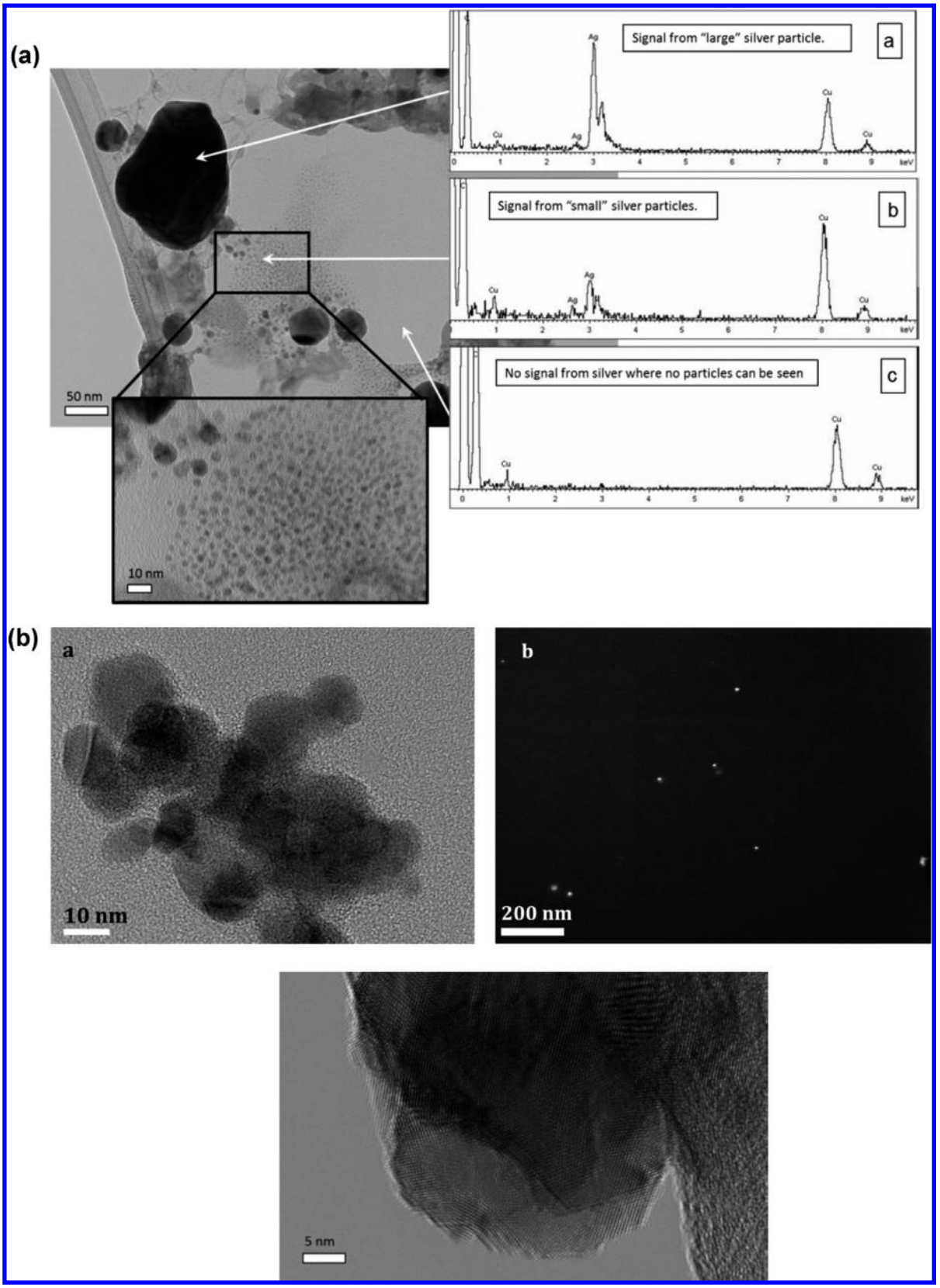

Figure 1. (a) Bright-field TEM image of Ag NPs in a water solution of pH 10 (sonicated and nonfiltered). Insets, based on EDS measurements in STEM mode, verify Ag in (a) large particles/agglomerates, (b) small particles, and in (c) no Ag identified in areas without visual particles. Signals also show carbon from the film and copper from the TEM grid. (b) Bright-field (a) and dark-field (b) TEM images of Ag NPs prepared by suspension in pH 10 solution followed by probe sonication, filtration, and drying on holey carbon-coated copper grids. The particles were verified as silver by EDS analysis. High-resolution TEM image (bottom).

dx.doi.org/10.1021/la4012873 | *Langmuir* 2013, 29, 8882−8891

oxygen-rich layer, which is in accordance with earlier findings by the authors.[7] When comparing the TEM images with PCCS findings it should be kept in mind that DLS is measuring the hydrodynamic size in solution rather than a silver core diameter in vacuum. It should also be noted that the silver dissolves to some extent in solution over time.[14,24] All stability studies presented below are based on filtered sample dispersions.

3.2. Ag NP Stability with Time in Water Solutions of pH 5.6 and pH 10. To assess the surface charge and agglomeration capability of Ag NPs in solution, changes in ζ-potential and particle size as a function of time and solution were monitored in a laundry-relevant aqueous solution without surfactants (pH 10) and in deionized water (pH 5.6), Figure 2.

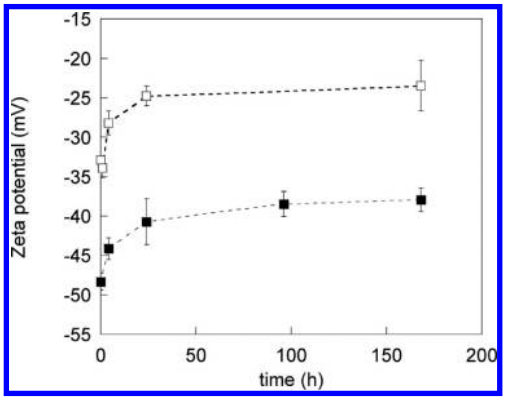

Figure 2. Changes in ζ-potential of Ag NPs as a function of time in deionized water (pH 5.6) (□) and in a laundry-relevant water solution without surfactants (adjusted to pH 10 by means of Na_2CO_3 and HNO_3) (■). Error bars represent the standard deviation within a single sample measured three times. Generated findings were verified for a selection of parallel samples. The lines are drawn for guidance only.

The Ag NPs showed negative surface potentials in both solutions independent of pH and exposure period. Measured ζ-potentials changed from initial values of −33 (pH 5.6) and −47 mV (pH 10) directly after preparation of the Ag NP dispersions, to relatively stable values of −25 and −40 mV, respectively, after 24 h. The major change (increase) in ζ-potential occurred in both solutions during the first 24 h and most drastically within the first 5 h followed by a nonsignificant change during subsequent time periods up to 1 week. An almost identical ζ-potential time dependence has been reported in the literature for chemically synthesized Ag NPs in water for which the ζ-potential increased from −45 to −39 mV during the first 4 h. This was attributed to surface adsorption of Ag^+ ions.[14] The observed surface charge was less negative in the solution of lowest pH (pH 5.6), findings in agreement with the literature for the same and other commercial and synthesized Ag NPs.[7,25,26] This is explained by the fact that more protons can coordinate with the particle surface in less alkaline solutions. Previous findings by the authors reveal negative surface potentials of the same Ag NPs at pH values higher than 3 (the isoelectric point) in pH-adjusted water solutions.[7] Transitions from negative to positive values of other Ag NPs in acidic water solutions of pH 2.7[26] and pH 1.5[25] have been reported. Colloidal metal particles in contact with water solutions develop a charge due to the adsorption of ions and/or by ionization of surface functional groups.[27] The reason for the observed negative charge of Ag NPs in solutions exceeding pH 3 may possibly be a result of a strong coordination of reversibly adsorbed oxygen[7] or of a strong coordination of nucleophilic molecules (water and OH^- ions) that donates electrons to the Ag NP surface.[15]

It is often stated for NPs in general that a particle suspension with a ζ-potential less than ±20 mV (in the absence of other stabilizing factors) is considered unstable and may result in particle sedimentation.[15] Findings of this study, Figure 2, show that the Ag NPs are sufficiently charged (>|20| mV) to avoid agglomeration and sedimentation and are stable also after 1 week in both solutions at given conditions.

3.3. Surface Charge and Ag NP Stability with Time in Water Solutions of pH 5.6 and pH 10: Effects of a Positively Charged Surfactant, DTAC. The absolute value of the ζ-potential of the negatively charged Ag NPs decreased with increased DTAC concentration in the water solution of pH 10 up to a critical DTAC concentration of 1 mM when the Ag NPs became neutralized by positively charged DTA^+, Figure 3. At this concentration, the net charge of the Ag NPs was slightly positive (+5 mV) 5 min after solution preparation. After 1 h of continued exposure, the net charge was slightly below zero (−3 mV), thus stable around zero. A contact period of 1 h between Ag NPs and surfactants may be representative for laundry cycle conditions.

The observed charge neutralization at 1 mM DTAC coincided with the formation of larger-sized particles/colloids,

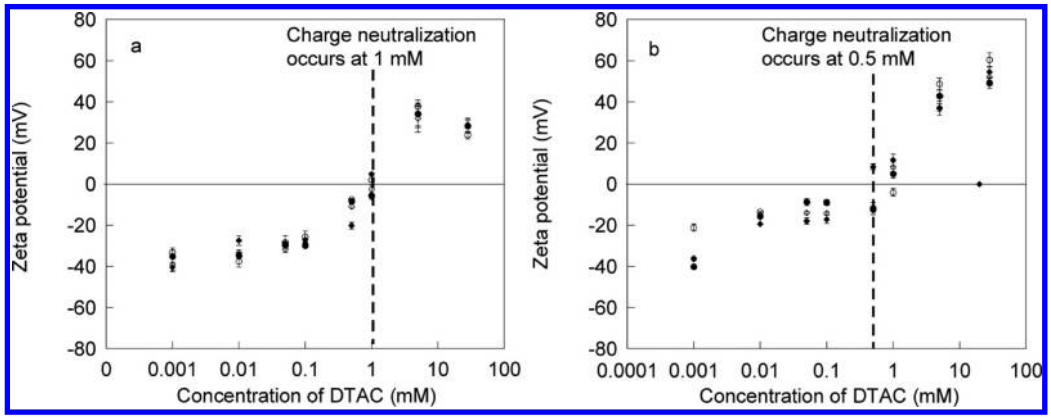

Figure 3. Changes in ζ-potential of Ag NPs with increased concentrations of DTAC (cmc approximately 20 mM) (0.001, 0.01, 0.05, 0.1, 0.5, 1, 5, or 28 mM) after 5 min (◆), 1 h (◊), 5 h (●), or 24 h (○) in a pH 10 water solution (a) and in deionized water of pH 5.6 (b). Error bars represent the standard deviation between duplicate samples measured two times each.

dx.doi.org/10.1021/la4012873 | Langmuir 2013, 29, 8882−8891

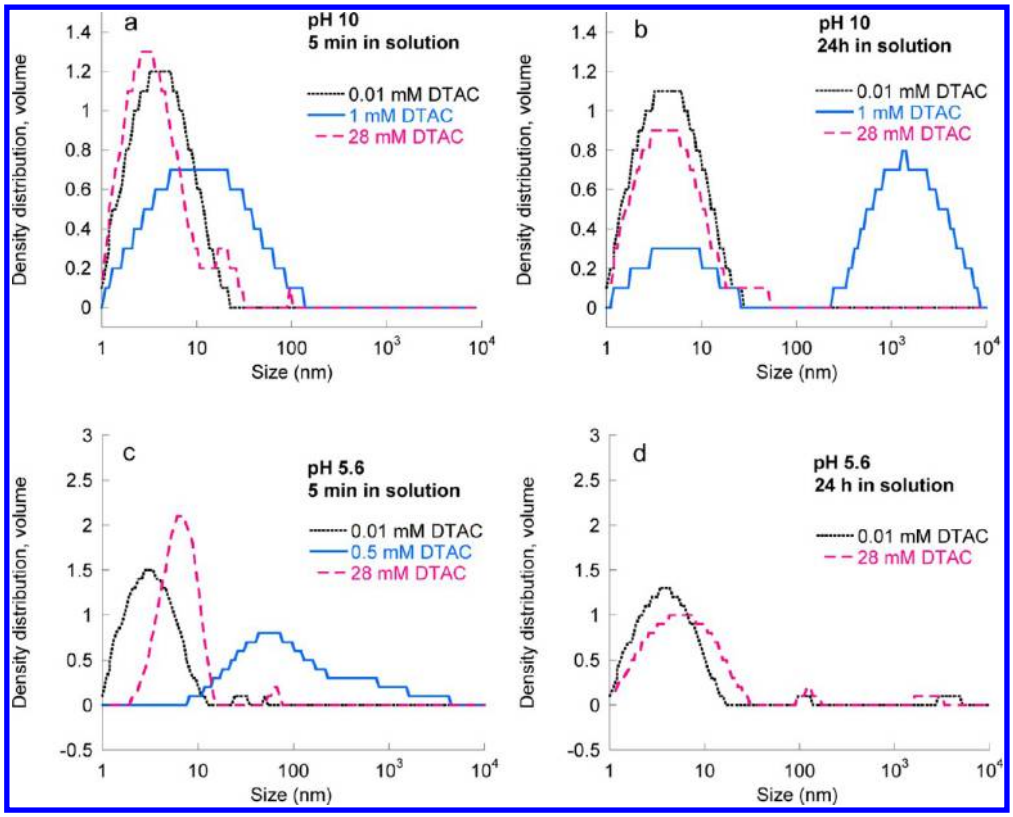

Figure 4. Particle size distribution measurements based and volume density of Ag NPs in aqueous solutions of pH 10 (a and b) and pH 5.6 (c and d), with different concentrations of DTAC after 5 min (a and c) and 24 h (b and d) of exposure.

as evident from PCCS findings in Figure 4, showing the volume density distribution of the particles. Particle size distributions based on number are shown in Figure S3 in the Supporting Information. The volume density more clearly shows the presence of larger agglomerates, and the number density provides information on the size of the majority of the particles.

The increased particle size with time (based on volume density) and the corresponding decreased absolute value of the ζ-potential (surface charge) upon DTAC addition (1 mM) were interpreted as the result of particle agglomeration, a process that influences the particle stability in solution. The reversal of the surface charge from negative to positive values observed at the highest DTAC concentrations investigated (5 and 28 mM) resulted in a reduced degree of agglomeration compared with 1 mM, Figure 4 (top). These high surfactant concentrations are believed to be the most relevant conditions of the laundry cycle (typically with surfactant concentrations above cmc).[20] The charge reversal is caused by surface adsorption of DTAC in a bilayer type structure due to a combination of electrostatic attraction between the oppositely charged Ag NP surfaces and DTAC and hydrophobic interactions between the surfactant tails. Since previous findings by the authors have shown other similar cationic surfactants (e.g., CTAB) to adsorb with their positively charged headgroup (trimethylammonium) oriented toward the Ag NP surface (based on surface-enhanced Raman scattering spectroscopy measurements, SERS), this was also believed to be the case for DTAC.[7]

Bilayer formation of cationic surfactants with disordered layer structures (or patchy bilayers) has previously been proposed for both negatively charged NPs and planar surfaces.[7,28−30] Adsorption of DTAC as a bilayer structure was furthermore supported by a 12-fold increase in sensed mass (from 0.1 to 1.2 mg/m^2) on evaporated QCM Ag sensors upon a 5-fold increase in concentration (0.1−0.5 mM) and a further 4-fold increase in sensed mass (to 4 mg/m^2) when increasing the concentration 10 times (0.5−5 mM) (Table S1 in the Supporting Information). It should be stressed that each Ag NP−surfactant solution was prepared separately and not via a continuous increase of the surfactant concentration, thus being comparable to PCCS and ζ-potential measurements for which the solutions were prepared in the same way.

For comparison, Ag NP−DTAC interactions were investigated in deionized water at pH 5.6 using the same surfactant concentrations as for the pH 10 solution, Figure 3. The results were essentially the same, except that a slightly lower DTAC concentration (0.5 mM) was required to reverse the surface charge from negative to positive compared with a required concentration of 1 mM DTAC in the pH 10 solution. This effect was attributed a lower surface charge (ζ-potential, see Figure 2) of the Ag NPs at pH 5.6 compared with pH 10. The ζ-potential increased already at the lowest DTAC concentration investigated (0.01 mM), a concentration far below cmc (20 mM). The major difference, compared to observed particle dynamics in the water solution of pH 10, was that no particle size distribution measurements (neither by volume nor by number) were possible after 24 h in the presence of DTAC at concentrations between 0.5 and 1 mM, Figure 4 (bottom). This is explained by the fact that the colloids at those concentrations are uncharged. Being uncharged makes them more prone to agglomerate and sediment from the solution, thus unavailable for detection. In 28 mM DTAC the particles were sufficiently charged (positively) to remain stable in solution despite the

dx.doi.org/10.1021/la4012873 | *Langmuir* 2013, 29, 8882−8891

higher ionic strength from the counterions in the solution, known to decrease particle stability.[31]

In order to further compare the findings with the theoretical stability of the agglomerates, DLVO calculations using the extended DLVO theory[31−33] were performed (equations and variables used and separate energy contributions are given in the Supporting Information, section S4 DLVO calculations and Figure S4). It is assumed that the stability of a colloidal system is decided by the attractive van der Waals forces, repulsive electrostatic forces, and possible steric forces (osmotic contribution) between the adsorbed surfactant layers.[27] However, between particles coated with a surfactant layer the range of the steric interaction (i.e., primarily between the headgroups) is rather short range due to the small size of the surfactant molecule. Stability calculations were performed for Ag NPs in (i) pure pH 10 water solution, (ii) pH 10 with 1 mM DTAC, and (iii) pH 10 with 28 mM DTAC, Figure 5.

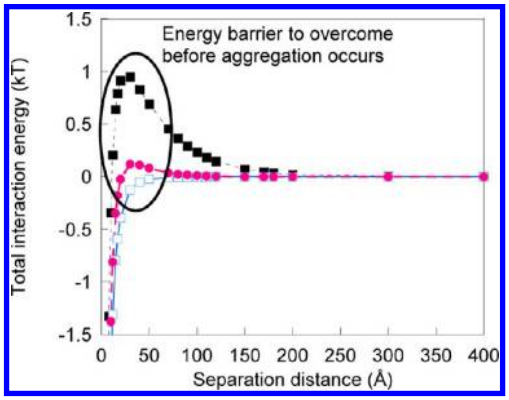

Figure 5. Total calculated interaction energies (kT) as a function of separation distance (Å) of Ag NPs in solutions of pH 10 water solution (■), pH 10 with 1 mM DTAC (□), and pH 10 with 28 mM DTAC (●).

Experimentally determined ζ-potentials of this study were used as input data. The calculations clearly show that the particles do not have any energy barrier for preventing agglomeration at 1 mM DTAC, whereas a barrier exists in the pure water solution and in the 28 mM DTAC solution, Figure 5. This supports the PCCS observations (Figure 4) demonstrating that the particles have agglomerated in the 1 mM DTAC solution. Furthermore, as expected, the calculations confirm that higher ionic concentrations result in a more unstable system.[31] This is indicated by the PCCS results in Figure 4, showing slightly more agglomerated particles for 28 mM DTAC compared with 0.01 mM, despite the fact that the particles were highly charged in both solutions (Figure 3). The increase in size for 28 mM DTAC compared with 0.01 mM could also partly be the result of an increased diameter due to the adsorbed surfactant layers onto the particles.

3.4. Surface Charge and Ag NP Stability with Time in Water Solutions of pH 5.6 and pH 10: Effects of a Nonionic Surfactant, Berol. The magnitude of the negative surface potential decreased with increased concentration of the nonionic surfactant Berol at higher concentrations (above cmc) and was almost neutralized at a concentration of 5 mM, Figure 6. Similar findings have earlier been shown by the authors in the presence of synthesized Ag NPs (both positively and negatively charged).[7] As expected, nonionic Berol by itself did not give rise to any measurable ζ-potential.[7]

Experimental findings on charge neutralization of charged particles by the interaction of nonionic surfactants such as Berol at high surfactant concentrations, see Figure 6, have not previously been reported. Findings in the literature rather state an unchanged, or minor reduction, in ζ-potential of charged particles in the presence of nonionic surfactants (e.g., Tween 80).[34] The ζ-potential is based on the mobility of a particle in an electric field and is related to the electric potential at the interface between the diffuse ion layer that surrounds the particle and the bulk solution, Figure 7a. Two possible explanations for the observed reduction in ζ-potential of negatively charged Ag NPs with increasing Berol concentration in a pH 10 solution (cf. Figure 6) are schematically illustrated in Figure 7. One possibility is that the relatively large bulky hydrophilic headgroup (ethoxyl) of adsorbed Berol moves the slipping plane (where the ζ-potential is measured) outward at high concentrations (Figure 7b) and hence results in a lower ζ-potential. Another possibility is that the adsorption of Berol gives rise to a more hydrophobic environment in the close proximity of the particle surface due to high concentrations of hydrocarbon from the tails of the surfactant close to the Ag NP surface (Figure 7d). This hydrophobic environment has a lower dielectric constant compared with conditions in Ag NP−water solutions without nonionic surfactants. Since a surface charge in hydrophobic environments is energetically unfavorable,[27] the observed reduction in surface charge of Ag NPs in the presence of Berol is reasonable. This is the most likely scenario, given the fact that these reported findings with minor reduction in ζ-

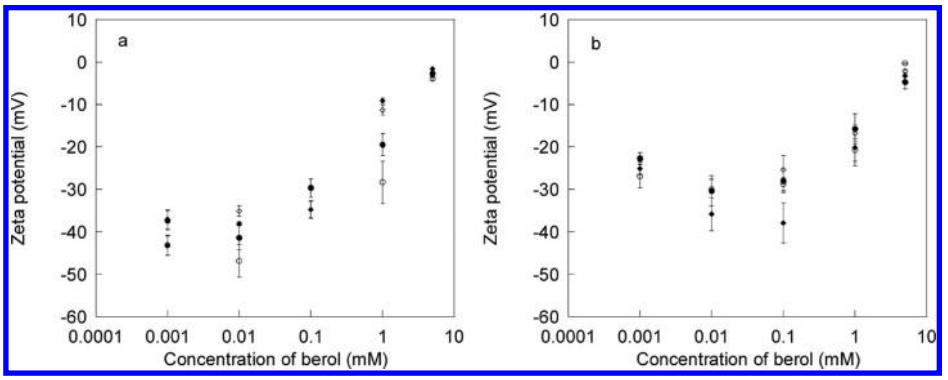

Figure 6. Changes in ζ-potential of Ag NPs interacting with different concentrations of Berol (cmc 0.075 mM) (0.001, 0.01, 0.1, 1, or 5 mM) in a pH 10 water solution (a) or in water of pH 5.6 (b) exposed for 5 min (◆), 1 h (◊), 5 h (●), and 24 h (○) after preparation. Error bars represent the standard deviation between duplicate samples measured two times each.

dx.doi.org/10.1021/la4012873 | Langmuir 2013, 29, 8882−8891

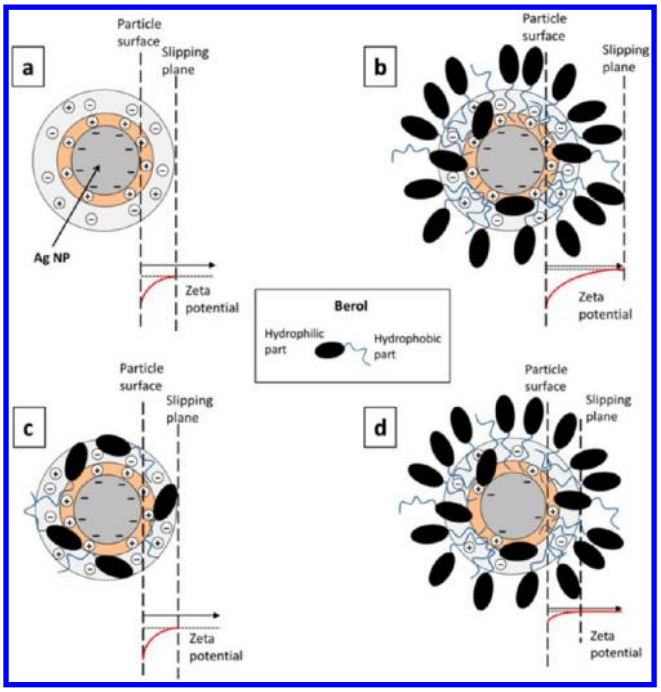

Figure 7. Schematic illustration of (a) the plane of surface charge (where the ζ-potential is measured) for Ag NPs, and its changes proposed for Berol adsorbed on Ag NPs at high surfactant concentration (>5 mM) due to (b) the movement of plane of charge or (d) the hydrophobicity at the NP/slipping plane interface. At lower concentrations Berol is expected to adsorb more irregularly (c).

potentials and lack of surfactant concentration dependence were based on 4 times larger surfactant concentrations (Tween 80) compared with the investigated concentrations of Berol in this study.[34] Despite these differences, only a minor reduction in surface charge of negatively charged Ag NPs (from −23 to −17 mV) with a 25-fold reduction in surfactant concentration (from 5 to 0.2 mM) was reported.[34] Since the same investigation reported an increased particle size due to adsorption of surfactants (from 57 to 76 nm), adsorption of Tween 80 most probably results in thicker adsorbed layers compared with the findings for Berol in this study. This adsorption process could move the plane of charge. However, similar to what was proposed for Berol above, the large size and bulky headgroup structure of Tween 80 may prevent the formation of a dense hydrophobic layer on the Ag NPs. This may explain the lack of reduction in surface charge due to Tween 80 adsorption,[34] as opposed to its observed reduction due to Berol adsorption in this study. At lower Berol concentrations the surfactants are expected to organize around the Ag NPs more randomly (Figure 7c) and not give rise to the same change in ζ-potential as for higher concentrations.

Adsorption studies were conducted on planar Ag QCM sensors by means of QCM to gain further understanding of the affinity of Berol to Ag, Figure 8. A 3.2-fold increase in sensed mass was observed when increasing the Berol concentration from 0.1 mM (2.8 mg/m^2) to 5 mM (9 mg/m^2).

The surface was probably saturated with Berol at a concentration of 5 mM since no significant change in sensed mass was taking place when increasing the concentration further to 10 mM. The sensed mass was relatively low at concentrations below 0.1 mM. These findings are consistent with literature findings showing surface adsorption of nonionic surfactants to generally increase at concentrations close to the

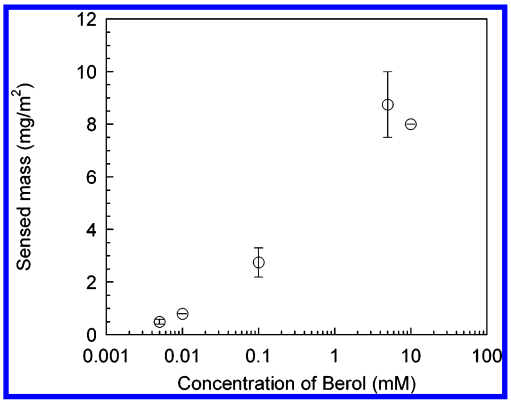

Figure 8. Change in sensed mass (QCM-D) for Ag sensors upon continuous addition of Berol from solutions of increased surfactant concentrations (0.005, 0.01, 0.1, 5, and 10 mM) in water (pH 5.6) Error bars represent the standard deviation between two independent measurements.

cmc (0.075 mM).[35,36] The sensed mass of Berol corresponded to an approximate thickness of 4 nm, i.e., one monolayer (cf. Supporting Information section S5). It is further important to note that the QCM technique measures the mass of the surface layer including water, which means that the mass measured with optical techniques of adsorbed Berol will be considerably lower than the sensed mass. Figure 8 indicates that the adsorption of Berol is cooperative, which is the result from the hydrogen bonds that attach the headgroups of the surfactant molecules to the surface. The mass is hence increasing cooperatively due to hydrophobic interaction between surfactant tails.

Berol has previously been shown to have a higher affinity for QCM Ag surfaces when adsorbed from a pure water solution (4.5 mg/m^2) compared with a pH 10 solution (2.5 mg/m^2).[7] The measured isoelectric point of a QCM Ag sensor was between pH 5 and 6 (data not shown). The estimated isoelectric point of the Ag NPs of this study was, however, lower (pH 3) than observed for the QCM sensor.[7]

The median particle size measured in solution (by number density, $d_{0.5}$) did not change upon increased Berol concentration, Figure 9a. The volume density on the other hand showed a small increase in $d_{0.5}$ when increasing the concentration of Berol to above 0.1 mM (Figure 9a). This is explained by a possible formation of larger agglomerates, as demonstrated in Figure 9c. Adsorption of Berol at the Ag NP surfaces at concentrations approximately above 0.1 mM increased the intensity of the scattered light (Figure 9b). The large error bars at high concentrations are explained by agglomeration, resulting in more polydisperse samples.

An increased scattered light intensity (Figure 9b) may often be interpreted as the formation of larger agglomerates, as larger particles scatter more light compared with small particles. Almost identical scattered light intensities were observed in pure solutions of Berol (without Ag NPs) of different concentration (1 and 5 mM) (cf. dotted line in Figure 9b). However, the results imply that the increase in scattered light intensity in 5 mM compared with 1 mM Berol, Figure 9b, is due to surface interactions of Berol, or to NP agglomeration, and not an effect of Berol forming larger structures in solution at increasing surfactant concentration. The indicated reduction intensity with time, particularly noticeable at a concentration of 5 mM Berol, is an effect of the settlement of a few larger

dx.doi.org/10.1021/la4012873 | Langmuir 2013, 29, 8882−8891

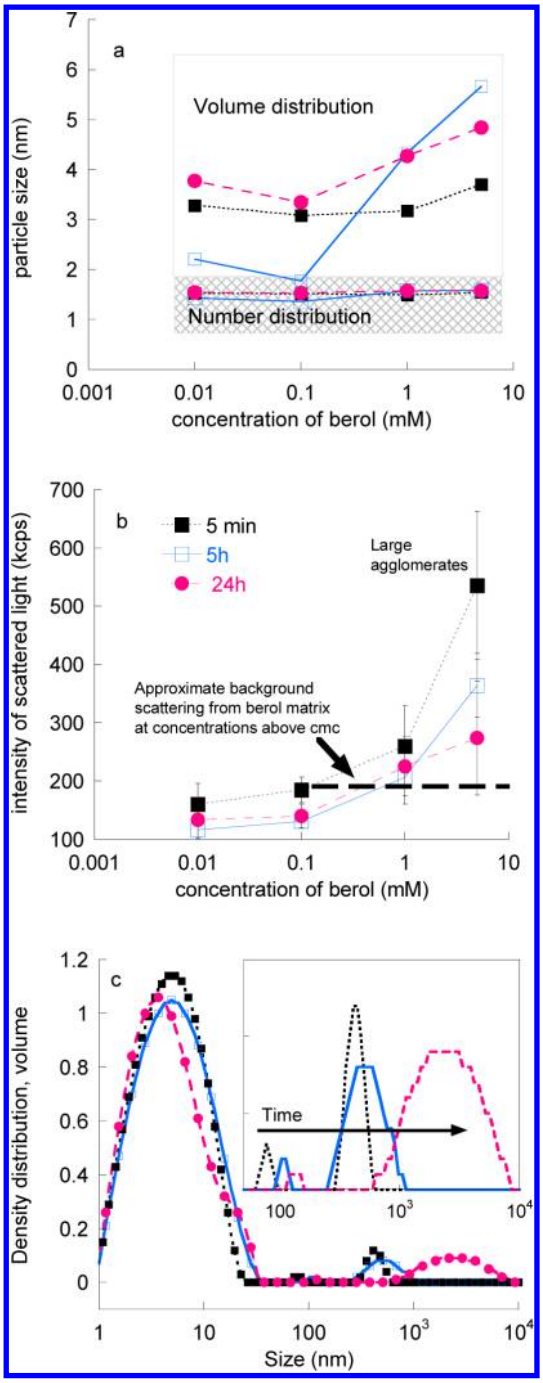

Figure 9. Particle median size ($d_{0.5}$) by number (bottom) and by volume (top) (a) and the intensity of the scattered light (b) of Ag NPs interacting with different concentrations of Berol (0.01, 0.1, 1, or 5 mM) in a pH 10 solution after immersion for 5 min (■), 5 h(□), or 24 h (●). The volume distributions of Ag NPs dispersed in 5 mM Berol are shown in panel c, indicating the formation of large agglomerates with time, with the inset being a magnification of the aggregates.

agglomerates (>100 nm) observed during the 24 h measurement, as confirmed by volume distribution data from PCCS measurements (Figure 9c). These agglomerates are believed to consist of Berol-adsorbed Ag NP agglomerates, as the increase in thickness of the Berol layer alone is too small (cf. QCM data above) to explain such large changes in size. The exact structure of the Berol layer will be further investigated with the more surface-sensitive technique, small-angle neutron scattering (SANS).

The results were compared with the DLVO theory as described in section 3.3 and Supporting Information section S4. The calculations were performed for Ag NPs in water solutions of (i) pH 10, (ii) pH 10 with 5 mM Berol, (iii) pH 5.6, and (iv) pH 5.6 with 5 mM Berol, Figure 10. The calculations clearly show that the presence of Berol in solution eliminates the energy barrier, why the particles will readily form agglomerates that may sediment. In solutions without surfactants, the calculations predict the presence of a small energy barrier sufficiently high to prevent immediate particle agglomeration. These calculations indicate that the contribution from the steric repulsion between the ethylene oxide headgroups at the solution−surface interface is not sufficient to compensate for the observed reduction in electrostatic stabilization of the particles. Hence, hydrophobic attraction between exposed surfactant tails creating hydrophobic patches on the surface will most likely also contribute to the agglomeration.

3.5. Surface Charge and Ag NP Stability with Time in Water Solutions of pH 5.6 and pH 10: Effects of a Negatively Charged Surfactant, LAS. The negative surface potential of Ag NPs increased with increased concentration of the negatively charged surfactant LAS, see Figure S5 in the Supporting Information. The interference of micelles of LAS on the measured ζ-potential at surfactant concentrations larger than 5 mM was considered negligible since no counts above background level were observed at surface potentials between −30 and −50 mV without the presence of NPs, which is in the range of measured ζ-potentials when Ag NPs are present. LAS alone only resulted in a small peak present at approximately −10 mV, cf. Figure S6 in the Supporting Information.

However, the possibility that LAS micelles contribute to the higher measured ζ-potential values at 5 mM (exceeding the cmc for LAS, 1.2 mM), Figure S6 in the Supporting Information, cannot be completely ruled out. No change in particle size was observed in the presence of LAS (cf. Supporting Information Table S2), and no interactions between LAS and Ag NPs were previously observed by SERS.[7] Very low amounts (<0.2 mg/m^2) of LAS were sensed on negatively charged QCM Ag sensors exposed to water solutions of pH 10 at low surfactant concentrations (0.1 mM). Significant amounts (2 mg/m^2) of LAS were sensed at high concentrations (5 mM, before rinsing) (cf. the Supporting Information, Figure S7). This adsorption is believed to be driven by hydrophobic interactions as negatively charged surfactants generally do not adsorb on very hydrophilic negatively charged surfaces such as, e.g., silica, due to strong electrostatic repulsion.[37] The negatively charged Ag NPs were stable in the presence of the negatively charged anionic surfactant LAS, without any changes in ζ-potential with respect to time, section S5 in the Supporting Information, or particle median size (based on both number and volume density, measured by means of PCCS, cf. Supporting Information Table S1) during 24 h of exposure in water solutions of pH 5.6 and pH 10.

4. CONCLUDING REMARKS

The adsorption of the cationic DTAC on Ag NPs resulted in a net charge reversal from a negative to a positive ζ-potential. Nontreated Ag NPs or particles previously in contact with LAS remained at negative ζ-potential values. Their stability was, however, strongly related to the ionic strength of the water

dx.doi.org/10.1021/la4012873 | Langmuir 2013, 29, 8882−8891

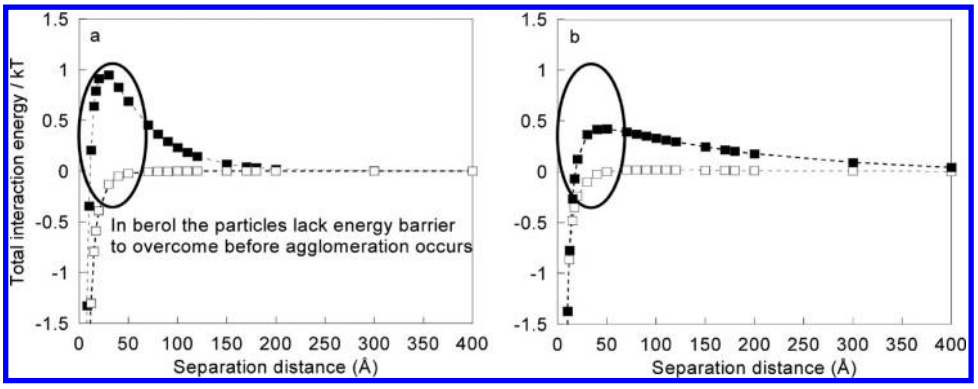

Figure 10. Total calculated interaction energies (V_{tot}) of Ag NPs in water solutions of pH 10 (a) and pH 5.6 (b) without surfactant (■) and with 5 mM Berol (5 mM) (□).

solution, which depended on the concentration of charged surfactants. At concentrations above 5 mM the nonionic Berol destabilized the particles in solution, which was consistent with the extended DLVO theory. The observations of a reduced ζ-potential of the Ag NPs after interaction with the nonionic Berol are novel and show that nonionic surfactants may change the electrostatic behavior of Ag NPs. It was proposed that adsorbed Berol either moved the slipping plane or created a more hydrophobic environment that resulted in a reduced ionization of surface charges. As a consequence, the particles were measured as uncharged.

This study showed that adsorption of surfactants (and/or surfactants present in solution) on Ag NPs modified their surface and either reduced or enhanced the degree of particle agglomeration depending on the type and concentration of the surfactant, as shown in this study. Predictions of the fate of potentially dispersed Ag NPs from consumer products, such as impregnated clothing, require an in-depth knowledge of interactions between surfactants of relevance for laundry formulations and Ag NPs. The assessment of changes in colloid stability and mobility upon transport to different chemical transients is also important. When entering a new chemical environment, the NPs will equilibrate with new ligands and may be further transported toward natural recipients. Depending on the reversibility of the surface modifications, the NPs may be transported with or without adsorbed surfactants or ligands of the given exposure setting.

■ ASSOCIATED CONTENT

Supporting Information

AFM and TEM pictures, PCCS data [both in form of graphs (for DTAC) and in form of a table (for LAS)], QCM and ζ-potential data for LAS, and details regarding the DLVO calculations and thickness of the surfactant layers. This material is available free of charge via the Internet at http://pubs.acs.org.

■ AUTHOR INFORMATION

Corresponding Author

*E-mail: sarasko@kth.se (S.S.); blev@kth.se (E.B.).

Notes

The authors declare no competing financial interest.

■ ACKNOWLEDGMENTS

Financial support from the Swedish Research Council, VR, and Formas is highly acknowledged. The authors are grateful to Malin Tornberg for assistance with the TEM measurements and to Esben Thormann for the AFM measurements.

■ REFERENCES

(1) Fabrega, J.; Luoma, S. N.; Tyler, C. R.; Galloway, T. S.; Lead, J. R. Silver nanoparticles: behaviour and effects in the aquatic environment. *Environ. Int.* **2011**, *37*, 517−531.

(2) Blaser, S. A.; Scheringer, M.; Macleod, M.; Hungerbühler, K. Estimation of cumulative aquatic exposure and risk due to silver: contribution of nano-functionalized plastics and textiles. *Sci. Total Environ.* **2008**, *390*, 396−409.

(3) Benn, T. M.; Westerhoff, P. Nanoparticle silver released into water from commercially available sock fabrics. *Environ. Sci. Technol.* **2008**, *42*, 4133−4139.

(4) Gottschalk, F.; Sonderer, T.; Scholz, R. W.; Nowack, B. Modeled environmental concentrations of engineered nanomaterials (TiO2, ZnO, Ag, CNT, fullerenes) for different regions. *Environ. Sci. Technol.* **2009**, *43* (24), 9216−9222.

(5) Geranio, L.; Heuberger, M.; Nowack, B. The behavior of silver nanotextiles during washing. *Environ. Sci. Technol.* **2009**, *43*, 8113−8118.

(6) Hogstrand, C.; Wood, C. M. Toward a better understanding of the bioavailability, physiology, and toxicity of silver in fish: Implications for water quality criteria. *Environ. Toxicol. Chem.* **1998**, *17* (4), 547−561.

(7) Hedberg, J.; Lundin, M.; Lowe, T.; Blomberg, E.; Wold, S.; Wallinder, I. O. Interactions between surfactants and silver nanoparticles of varying charge. *J. Colloid Interface Sci.* **2012**, *369*, 193−201.

(8) Nowack, B.; Ranville, J. F.; Diamond, S.; Gallego-Urrea, J. A.; Metcalfe, C.; Rose, J.; Horne, N.; Koelmans, A. A.; Klaine, S. J. Potential scenarios for nanomaterial release and subsequent alteration in the environment. *Environ. Toxicol. Chem.* **2012**, *31* (1), 50−59.

(9) Levard, C.; Hotze, E. M.; Lowry, G. V.; Brown, G. E. Environmental transformations of silver nanoparticles: Impact on stability and toxicity. *Environ. Sci. Technol.* **2012**, *46* (13), 6900−6914.

(10) Li, X.; Lenhart, J. J.; Walker, H. W. Aggregation kinetics and dissolution of coated silver nanoparticles. *Langmuir* **2012**, *28* (2), 1095−1104.

(11) Marambio-Jones, C.; Hoek, E. A review of the antibacterial effects of silver nanomaterials and potential implications for human health and the environment. *J. Nanopart. Res.* **2010**, *12* (5), 1531−1551.

(12) Kvitek, L.; Panacek, A.; Soukupova, J.; Kolar, M.; Vecerova, R.; Prucek, R.; Holecova, M.; Zboril, R. Effect of surfactants and polymers on stability and antibacterial activity of silver nanoparticles (NPs). *J. Phys. Chem. C* **2008**, *112* (15), 5825−5834.

(13) Mukherjee, B.; Weaver, J. W. Aggregation and charge behavior of metallic and nonmetallic nanoparticles in the presence of competing similarly-charged inorganic ions. *Environ. Sci. Technol.* **2010**, *44* (9), 3332−3338.

(14) Liu, J.; Hurt, R. H. Ion release kinetics and particle persistence in aqueous nano-silver colloids. *Environ. Sci. Technol.* **2010**, *44*, 2169−2175.
(15) El Badawy, A. M.; Luxton, T. P.; Silva, R. G.; Scheckel, K. G.; Suidan, M. T.; Tolaymat, T. M. Impact of environmental conditions (pH, ionic strength, and electrolyte type) on the surface charge and aggregation of silver nanoparticles suspensions. *Environ. Sci. Technol.* **2010**, *44* (4), 1260−1266.
(16) Pungor, E.; Toth, K.; Hrabeczypall, A. Selectivity coefficients of ion-selective electrodes. *Pure Appl. Chem.* **1979**, *51*, 1915−1980.
(17) Whitlow, S. I.; Rice, D. L. Silver complexation in river waters of central New York. *Water Res.* **1985**, *19* (5), 619−626.
(18) Rogers, K. R.; Bradham, K.; Tolaymat, T.; Thomas, D. J.; Hartmann, T.; Ma, L.; Williams, A. Alterations in physical state of silver nanoparticles exposed to synthetic human stomach fluid. *Sci. Total Environ.* **2012**, *420* (0), 334−339.
(19) MacCuspie, R. I.; Allen, A. J.; Hackley, V. A. Dispersion stabilization of silver nanoparticles in synthetic lung fluid studied under in situ conditions. *Nanotoxicology* **2011**, *5* (2), 140−156.
(20) Smulders, E.; Rybinski, W.; Sung, E.; Rähse, W.; Steber, J.; Nordskog, A. Laundry Detergents. *Ullmann's Encyclopedia of Industrial Chemistry* [CD-ROM]; Wiley-VCH: Weinheim, Germany, 2007.
(21) Kaegi, R.; Voegelin, A.; Sinnet, B.; Zuleeg, S.; Hagendorfer, H.; Burkhardt, M.; Siegrist, H. Behavior of metallic silver nanoparticles in a pilot wastewater treatment plant. *Environ. Sci. Technol.* **2011**, *45* (9), 3902−3908.
(22) Sauerbrey, G. Verwendung von schwingquarzen zur wägung dünner schichten und zur mikrowägung. *Z. Phys. A: Hadrons Nucl.* **1959**, *155* (2), 206−222.
(23) Taurozzi, J. S.; Hackley, V. A.; Wiesner, M. R. A standardised approach for the dispersion of titanium dioxide nanoparticles in biological media. *Nanotoxicology* **2013**, *7* (4), 389−401.
(24) Liu, J.; Sonshine, D. A.; Shervani, S.; Hurt, R. H. Controlled release of biologically active silver from nanosilver surfaces. *ACS Nano* **2010**, *4*, 6903−6913.
(25) Elzey, S.; Grassian, V. H. Agglomeration, isolation and dissolution of commercially manufactured silver nanoparticles in aqueous environments. *J. Nanopart. Res.* **2010**, *12* (5), 1945−1958.
(26) Alvarez-Puebla, R. A.; Arceo, E.; Goulet, P. J. G.; Garrido, J. J.; Aroca, R. F. Role of nanoparticle surface charge in surface-enhanced Raman scattering. *J. Phys. Chem. B* **2005**, *109* (9), 3787−3792.
(27) Evans, D. F.; Wennerström, H. *The Colloidal Domain: Where Physics, Chemistry, Biology and Technology Meet*, 2nd ed.; John Wiley & Sons: New York, 1999.
(28) Sui, Z.; Chen, X.; Wang, L.; Chai, Y.; Yang, C.; Zhao, J. An improved approach for synthesis of positively charged silver nanoparticles. *Chem. Lett.* **2005**, *34*, 100−101.
(29) Sui, Z.; Chen, X.; Wang, L.; Xu, L.; Zhuang, W.; Chai, Y.; Yang, C. Capping effect of CTAB on positively charged Ag nanoparticles. *Phys. E (Amsterdam, Neth.)* **2006**, *33*, 308−314.
(30) Penfold, J.; Staples, E. J.; Tucker, I.; Thomas, R. K. Adsorption of mixed cationic and nonionic surfactants at the hydrophilic silicon surface from aqueous solution: The effect of solution composition and concentration. *Langmuir* **2000**, *16* (23), 8879−8883.
(31) Stebounova, L. V.; Guio, E.; Grassian, V. H. Silver nanoparticles in simulated biological media: A study of aggregation, sedimentation, and dissolution. *J. Nanopart. Res.* **2011**, *13*, 233−244.
(32) Shah, P. S.; Holmes, J. D.; Johnston, K. P.; Korgel, B. A. Size-selective dispersion of dodecanethiol-coated nanocrystals in liquid and supercritical ethane by density tuning. *J. Phys. Chem. B* **2002**, *106* (10), 2545−2551.
(33) Vincent, B.; Edwards, J.; Emmett, S.; Jones, A. Depletion flocculation in dispersions of sterically-stabilized particles (soft spheres). *Colloids Surf.* **1986**, *18* (2−4), 261−281.
(34) Soukupová, J.; Kvítek, L.; Panáček, A.; Nevěčná, T.; Zbořil, R. Comprehensive study on surfactant role on silver nanoparticles (NPs) prepared via modified Tollens process. *Mater. Chem. Phys.* **2008**, *111* (1), 77−81.
(35) Brinck, J.; Jönsson, B.; Tiberg, F. Kinetics of nonionic surfactant adsorption and desorption at the silica−water interface: One component. *Langmuir* **1998**, *14* (5), 1058−1071.
(36) Tiberg, F.; Brinck, J.; Grant, L. Adsorption and surface-induced self-assembly of surfactants at the solid−aqueous interface. *Curr. Opin. Colloid Interface Sci.* **1999**, *4* (6), 411−419.
(37) Bastardo, L. A.; Iruthayaraj, J.; Lundin, M.; Dedinaite, A.; Vareikis, A.; Makuska, R.; van der Wal, A.; Furo, I.; Garamus, V. M.; Claesson, P. M. Soluble complexes in aqueous mixtures of low charge density comb polyelectrolyte and oppositely charged surfactant probed by scattering and NMR. *J. Colloid Interface Sci.* **2007**, *312* (1), 21−33.